Solid–Liquid Catalytic Reactions in a New Two-Impinging-Jets Reactor: Experiment and Modeling

ARTICLE *in* INDUSTRIAL & ENGINEERING CHEMISTRY RESEARCH · MARCH 2009

Impact Factor: 2.59 · DOI: 10.1021/ie801240q

3 AUTHORS:

Asghar Molaei
Tabriz Islamic Art University
30 PUBLICATIONS **216** CITATIONS
SEE PROFILE

Iman Safari
Illinois Institute of Technology
16 PUBLICATIONS **70** CITATIONS
SEE PROFILE

Amirali Ebrahimi
University of Sydney
11 PUBLICATIONS **30** CITATIONS
SEE PROFILE

Article

Solid#Liquid Catalytic Reactions in a New Two-Impinging-Jets Reactor: Experiment and Modeling

Asghar Molaei Dehkordi, Iman Safari, and Amir A. Ebrahimi

Ind. Eng. Chem. Res., **Article ASAP** • DOI: 10.1021/ie801240q • Publication Date (Web): 12 February 2009

Solid−Liquid Catalytic Reactions in a New Two-Impinging-Jets Reactor: Experiment and Modeling

Asghar Molaei Dehkordi,* Iman Safari, and Amir A. Ebrahimi

Department of Chemical and Petroleum Engineering, Sharif University of Technology, P.O. Box 11155-9465, Tehran, Iran

Novel type of two-impinging-jets loop reactor (TIJLR) has been proposed and tested successfully for the solid−liquid catalytic reactions. The TIJLR was tested using the catalytic reaction of isomerization of D-glucose to D-fructose by immobilized glucose isomerase catalyst as a typical model system of solid−liquid catalytic reactions. The TIJLR is characterized by a high intensity reaction chamber, which is separated by a perforated plate from other parts of the reactor. The perforated plate was used as a filter to keep the catalyst particles within the reaction chamber. A compartment model with two adjustable parameters was considered to describe the pattern of flow within the reaction chamber. The compartment model proposed was based on the observation made during the experimental work. The adjustable parameters of the proposed model were determined through the experimental data by minimizing the discrepancies between the model predictions and corresponding experimental data. The influences of various operating and design parameters such as jet Reynolds number, feed flow rate, initial feed concentration, catalyst loading, and the volume of the reaction chamber on the performance capability of the TIJLR were investigated. It was found that the jet Reynolds number plays an important role in the performance capability of the TIJLR.

1. Introduction

Solid−liquid catalytic reactions are widely used in chemical industries. The industrial applications of solid−liquid catalytic reactions are extensive. For example, solid−liquid enzyme reactions constitute important processes in biochemical industries. Among the latter, the isomerization of glucose to fructose is one of the most widely used processes in the food industry in producing dietetic "light" foods and drinks because it improves the sweetening, color, and hygroscopic characteristics in addition to reducing viscosity. In addition, fructose is about 75% sweeter than sucrose, is absorbed more slowly than glucose, and is metabolized without the intervention of insulin. For all these reasons, this process is widely studied both with cells and with enzymes, both free and immobilized (IE).[1−20] From the perspective of chemical kinetics, isomerization of glucose to fructose is a reversible reaction, with an equilibrium constant of approximately unity at 55 °C.[16] The heat of reaction is on the order of 5 kJ mol^{-1},[4] and consequently, the equilibrium product contains roughly a 1:1 ratio of glucose to fructose that does not change significantly with reaction temperature, such that at 55 °C the fructose content at equilibrium is 50%, and at higher temperatures such as 60, 70, 80, and 90 °C is 50.7, 52.5, 53.9, and 55.6%, respectively. However, increasing temperature decreases stability and the enzyme half-life and, therefore, productivity. Most industrial plants run at 58−60 °C, a temperature with low risk for microbial contamination.

The process was originally carried out in batch reactors with soluble enzymes. It was later extended to one involving immobilized glucose isomerase (IGI), which is of interest to us in the present work. In addition to the aforementioned batch reactors, there are various types of enzyme reactors, including continuous stirred tank reactors (CSTR), fixed-bed reactors, simulated moving beds,[17] and fluidized-bed reactors. In the fixed- and fluidized-bed reactors, the immobilized enzymes are used with different shapes including cylindrical and spherical pellets. Because the microporous particles provide a large surface area and as packing such particles in a tubular reactor is rather straightforward, tubular packed-bed reactors consisting of IGI catalyst are extensively used. Isomerization of glucose to fructose is normally carried out in multiple tubular packed-bed reactors in parallel lines with an isomerization time ranging from 0.5 to 4 h.[16]

The impinging jets (IJ) technique is a unique flow configuration. The first patent for this technique was published by Bower.[21] The IJ technique was used by Elperin[22] for gas−solid suspensions and further developed by Tamir[23] in various chemical engineering processes. The IJ technique has been successfully applied to various chemical processes such as desorption,[24] absorption,[25−28] solid−liquid enzyme reactions,[29] copper extraction and stripping,[30,31] liquid−liquid reactions,[32,33] precipitation,[34,35] and crystallization with a calcium oxalate model system.[36]

The main objectives of the present work were as follows: (1) To investigate the application of a new type of two-impinging-jets loop reactor in solid−liquid catalytic reactions. (2) To model the proposed reactor using a compartmental-modeling approach. (3) To investigate the influences of various operating and design parameters on the performance capability of the proposed reactor.

To achieve the above goals, an investigation on the catalytic isomerization of glucose to fructose as a typical model system of solid−liquid catalytic reactions, applying a new two-impinging-jets loop reactor (TIJLR), has been investigated.

2. Reaction Kinetics

Glucose-fructose enzymatic isomerization is a reversible reaction and is normally given by the following expression:

$$G + E \underset{k_{-1}}{\overset{k_1}{\rightleftharpoons}} GE \underset{k_{-2}}{\overset{k_2}{\rightleftharpoons}} F + E \qquad (1)$$

where G, E, and F represent glucose, enzyme, and fructose, respectively, and GE is an intermediate complex formed during

* To whom correspondence should be addressed. E-mail: amolaeid@sharif.edu. Tel.: +98-21-66165412. Fax: +98-21-66022853.

10.1021/ie801240q CCC: $40.75

Table 1. Kinetic Constants of eq 7

$[G]_0$ (mol m^{-3})	K	$K_r \times 10^6$ (mol g_{cat}^{-1} s^{-1})
100	−0.070	2.991
500	−0.206	9.390
1000	−0.244	11.460
1250	−0.335	12.530

Table 2. Kinetic Parameters of eq 2

k_{mg} (mol m^{-3})	k_{mf} (mol m^{-3})	$v_{mg} \times 10^6$ (mol g_{cat}^{-1} s^{-1})	$v_{mf} \times 10^6$ (mol g_{cat}^{-1} s^{-1})
474.3	793.9	8.869	14.910

the reaction. According to the reversible modified Michaelis−Menten mechanism,[2,8,18,19] the reaction rate is given by

$$R = -\frac{1}{W}\frac{d[\bar{G}]}{dt} = \frac{V_m[\bar{G}]}{K_m + [\bar{G}]} \tag{2}$$

with

$$[\bar{G}] = [G] - [G]_e, \quad [G]_0 = [G] + [F] = [G]_e + [F]_e = (1 + K_e)[G]_e = (1 + K_e^{-1})[F]_e \tag{3}$$

$$K_m = \frac{k_{mf}k_{mg}}{k_{mf} - k_{mg}}\left[1 + \left(\frac{1}{k_{mg}} + \frac{K_e}{k_{mf}}\right)[G]_e\right] \tag{4}$$

$$V_m = [1 + K_e^{-1}]\frac{k_{mf}v_{mg}}{k_{mf} - k_{mg}} \tag{5}$$

$$K_e = \frac{[F]_e}{[G]_e} = \frac{X_e}{1 - X_e} = \frac{v_{mg}k_{mf}}{v_{mf}k_{mg}} \tag{6}$$

where v_{mg}, v_{mf}, k_{mg}, and k_{mf} are the maximum reaction rate for glucose to fructose, the maximum reaction rate for fructose to glucose, the Michaelis−Menten constant for glucose to fructose reaction, and the Michaelis−Menten constant for fructose to glucose reaction, respectively, and X_e is the equilibrium fractional conversion of glucose. In addition, the reaction rate expression could be given by[1]

$$R = -\frac{1}{W}\frac{d[G]}{dt} = K_r\frac{(X_e - X)}{1 + KX} \tag{7}$$

with

$$K_r = \frac{v_{mg}(1 + K_e^{-1})}{k_{mg} + [G]_0}[G]_0 \tag{8}$$

and

$$K = \frac{[G]_0\left[\left(\frac{K_{mg}}{K_{mf}}\right) + 1\right]}{k_{mg} + [G]_0} \tag{9}$$

where K_e, W, and X denote the equilibrium constant, catalyst loading, and the fractional conversion of glucose, respectively. Dehkordi et al.[1] have reported the values of kinetic parameters and the equilibrium fractional conversion of glucose to fructose isomerization reaction with the Sweetzyme IT as the catalyst at the reaction temperature of 60 °C, which are summarized in Tables 1 and 2. As an approximation, the reaction rate of glucose to fructose isomerization may be given by a pseudo-first-order rate expression as follows:

$$R = -\frac{1}{W}\frac{d[G]}{dt} \cong K_r(X_e - X) \tag{10}$$

Table 3. Physical Properties at 60 °C

initial glucose concentration (mol m^{-3})	ρ (kg m^{-3})	$\mu \times 10^4$ (kg m^{-1} s^{-1})
100	987.2	7.8
470	1008.5	8.1
880	1039.2	8.5
1100	1054.2	8.8

This rate expression could be valid when the product of $KX \ll 1$.

3. Experimental Section

3.1. Chemicals. All chemicals used in the present investigation were of analytical grade; D-glucose in crystalline form was supplied by Merck Co. (Germany). The immobilized enzyme, Sweetzyme IT, was provided as a gift by Novo Nordisk (Iran). The immobilized glucose isomerase (IGI) enzyme particles were of cylindrical shape, with 0.2−0.4 mm diameter, 1−1.5 mm length, and a particle density of 3300 kg m^{-3}. The dry specific activity of the IGI enzyme was reported to be 450 IGIU g^{-1} by the manufacturer. The distilled water used had a conductivity ≤ 3 μS cm^{-1}.

3.2. Method of Analysis. Fructose and glucose concentrations were determined by HPLC (Waters, refractive index detector 2410). The sugar pack1 column was used with deionized water as the mobile phase at a flow rate of 0.34 mL min^{-1}. The HPLC detector was calibrated by introducing known samples of D-glucose and D-fructose solutions. The regression coefficient of the calibration curve of the detector was 0.996.

The accuracy of the above-mentioned analytical method was examined using known samples of D-glucose and D-fructose solutions. From these tests, the errors of the analytical methods were found to be within the range of ±1%.

The viscosity of feed solutions at 60 °C and at various concentrations was determined by a viscometer (Boorkfield LVSVE 230), and the density of these solutions was determined by a density meter (Anton Paar DMA 38). The physical properties of glucose solution at 60 °C are listed in Table 3.

3.3. Experimental Apparatus. The flow diagram of the experimental setup, shown in Figure 1, consisted of the following parts: two-impinging-jets reactor whose dimensions were specified in Figure 1 (1); reaction chamber with varying volume (2); perforated plate in order to keep the catalyst particles within the reaction chamber and to prevent the catalyst particles from exiting the reaction chamber (3); rotameter in order to adjust the volumetric flow rate of the feed solution (4); feed pump made of stainless steel (SS) with the capacity of 40 L min^{-1} (5); feed vessel made of SS with the dimensions given in Figure 1 (6), which was equipped with a jacket (7); and a sampling connection (8). Using this configuration the volume of reaction chamber could be varied by moving the perforated plate along the reactor length.

3.4. Experimental Procedure. The D-glucose solution was prepared by dissolving the required amount of D-glucose in a solution containing 2.465 g of $MgSO_4 \cdot 7H_2O$ per liter of deionized water to stabilize the enzyme; the pH of the solution was adjusted at 7.5 by Na_2CO_3. Because oxygen in the syrup inactivates the enzyme and is responsible for increased formation of secondary products during isomerization, a low oxygen tension has to be achieved by adding Na_2SO_3.

In each experimental run, the desired amount of catalyst was added to the reaction chamber of the reactor and then the perforated plate was fitted in the reaction chamber so that the volume of the reaction zone was set to a given value. The feed

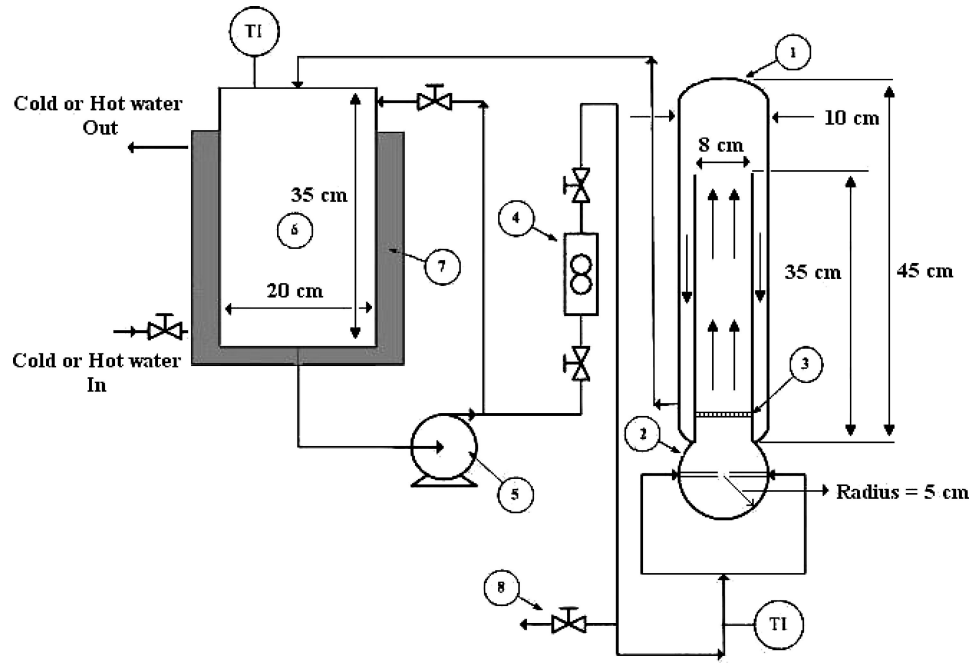

Figure 1. Experimental setup: (1) TIJLR; (2) reaction chamber; (3) perforated plate; (4) rotameter; (5) stainless steel feed pump; (6) stainless steel feed vessel; (7) hot water jacket; (8) sampling connection; TI = temperature indicator.

solution prepared according to the aforementioned procedure was introduced into the feed vessel while hot water was introduced into the jacket to keep the temperature of the feed at 60 °C. The feed solution at a given volumetric flow rate regulated using the rotameter was continuously fed to the reactor. This time was considered as the "zero time" of the reaction for the experimental records. A recycled stream from the discharge of the feed pump was also used to homogenize the entire content of the feed vessel. It should be added that preliminary measurements of concentration of glucose solution within the feed vessel and that exiting the rotameter showed that such a setup results in the uniform concentration of glucose within the feed vessel. The effluent of the reaction chamber after being passed through the perforated plate to separate the solid catalyst, moves along the reactor height, and overflows to the external zone of the reactor and then was recycled to the feed vessel. The samples were taken through the sampling connection for the measurement of glucose−fructose concentrations. The progress of the reaction within the sampling bottles was immediately ceased by adding an appropriate amount of sulfuric acid solution. Analysis of the samples was performed by the aforementioned analytical method for the glucose−fructose concentrations.

The reproducibility of the experimental results was also checked so that for each data point, the experimental run was repeated at least two times. Thus, each data point was determined based on the mean value of at least two measurements of glucose−fructose concentrations with a standard deviation of 1−2% and a mean deviation of 1.3% for all the experiments.

4. Results and Discussion

The operating and design conditions used in the present investigation for the determination of glucose conversion are summarized in Table 4. In the present investigation, the effects of important design and operating parameters on the performance capability of the proposed reactor were investigated. These parameters were the feed flow rate, jet diameter, initial

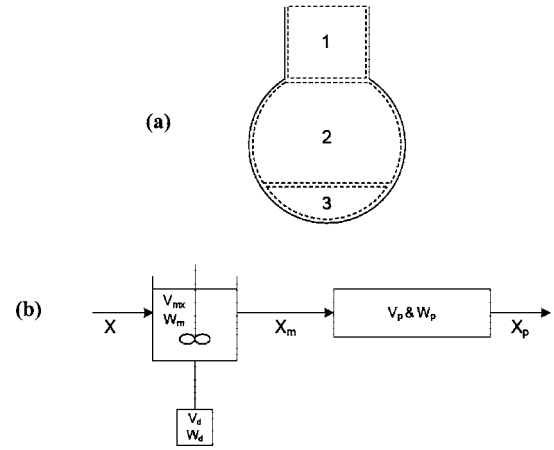

Figure 2. Model of the TIJLR. (a) Flow regions proposed for the TIJLR: 1 = plug flow region; 2 = mixed flow region; 3 = stagnant region. (b) The resulting model: mx, perfect mixed region; p: perfect plug region; and d, stagnant region.

Table 4. Operating and Design Conditions of Experimental Runs

internozzle distance (mm)	10
operating temperature (°C)	60 ± 1
pH of glucose solution	7.5
initial glucose concentration (kmol m^{-3})	0.1−1.25
feed flow rate (dm^3 min^{-1})	2.0−9.0
jet diameter (mm)	2−4
catalyst loading (g dm^{-3})	5−20
reaction zone volume (mL)	550−1350

concentration of glucose solution, reaction chamber volume, and the catalyst loading. In what follows the influences of these important operating and design parameters on the performance capability of the TIJLR are presented and discussed.

4.1. Reactor Model. To model the TIJLR, a compartment model was devised to comply with the pattern of flow within the reaction chamber. Figure 2 shows the proposed compartment model, which consists of the following regions: (1) a perfect plug flow region with the volume of V_p and the amount of solid catalyst of W_p; (2) a perfect mixed region with the volume of

Table 5. Effect of f_p on the Calculated Glucose Conversion at t = 160 min[a]

f_p	f_m	f_d	X_{cal}
0.0	1.0	0	0.3075
0.1	0.9	0	0.3076
0.2	0.8	0	0.3077
0.3	0.7	0	0.3077
0.5	0.5	0	0.3078
0.8	0.2	0	0.3079
0.9	0.1	0	0.3079

[a] $[G]_0$ = 1250 mol m^{-3}; V_r = 550 mL; catalyst loading = 10 g dm^{-3}; feed flow rate = 8 dm^3 min^{-1}.

V_{mx} and the amount of solid catalyst of W_m; and finally (3) a stagnant region with the volume of V_d and the amount of solid catalyst of W_d. Let the time varying fractional conversion of glucose at the inlet of the perfect mixed region, outlet of the perfect mixed region, and the outlet of the perfect plug flow region to be X, X_m, and X_p, respectively. According to this notation, we have

$$W = W_m + W_d + W_p \tag{11}$$

$$V_r = V_{mx} + V_d + V_p \tag{12}$$

where W and V_r are the total amount of solid catalyst within the reaction chamber and the total volume of the reaction chamber, respectively.

The glucose mass balance equation applied to the perfect mixed region (i.e., an ideal CSTR) yields

$$q[G]_0(1 - X) - q[G]_0(1 - X_m) = RW_m \tag{13}$$

where q is the volumetric flow rate of glucose solution and R can be given by eq 10. Substituting the pseudo-first-order rate expression of glucose isomerization (eq 10) in eq 13 yields

$$q[G]_0(X_m - X) = K_r(X_e - X_m)W_m \tag{14}$$

Solving for X_m where

$$\alpha = \frac{X_e}{1 + \dfrac{q[G]_0}{K_r W_m}} \tag{15}$$

$$\beta = \frac{1}{1 + \dfrac{K_r W_m}{q[G]_0}} \tag{16}$$

we get

$$X_m = \alpha + \beta X \tag{17}$$

For the perfect plug flow region, a differential mass balance along the plug flow region (i.e., z) gives

$$-q[G]_0 \frac{d(1 - X)}{dz} = R\frac{W_p}{V_p}A \tag{18}$$

where A is the cross-section area of the plug flow region. Substituting R into eq 18 gives

$$q[G]_0 \frac{dX}{dz} = K_r(X_e - X)\frac{W_p}{V_p}A \tag{19}$$

On integration with $X = X_m$, $z = 0$, and $X = X_p$, $z = Z_p$ where Z_p is the length of the plug flow region, we have

$$\ln \frac{X_e - X_m}{X_e - X_p} = \frac{K_r W_p}{q[G]_0} \tag{20}$$

or

$$\frac{X_e - X_m}{X_e - X_p} = \exp\left(\frac{K_r W_p}{q[G]_0}\right) \tag{21}$$

Letting

$$A = \frac{K_r W_p}{q[G]_0} \tag{22}$$

leads to

$$X_e - X_p = (X_e - X_m)\exp(-A) \tag{23}$$

Substituting X_m by eq 17 in eq 23 and solving for X_p gives

$$X_p = X_e[1 - \exp(-A)] + \alpha \exp(-A) + \beta \exp(-A)\, X \tag{24}$$

The glucose mass balance applied on the whole system yields

$$V\frac{dX}{dt} = q(X_p - X) \tag{25}$$

where V is the total volume of glucose solution in the reactor. By combining eqs 24 and 25 we obtain

$$\frac{V}{q}\frac{dX}{dt} = \gamma + \eta X \tag{26}$$

where

$$\gamma = X_e[1 - \exp(-A)] + \alpha \exp(-A) \tag{27}$$

and

$$\eta = \beta \exp(-A) - 1 \tag{28}$$

Integrating eq 26 with $X = 0$, $t = 0$ and $X = X$, $t = t$, yields

$$\ln\left(1 + \frac{\eta}{\gamma}X\right) = \frac{\eta q}{V}t \tag{29}$$

Solving for X gives

$$X = \frac{\gamma}{\eta}\left[\exp\left(\frac{\eta q}{V}t\right) - 1\right] \tag{30}$$

Letting $W_p = f_p W$ and $W_d = f_d W$, the resulting model is a model with two adjustable parameters that could be adjusted through experimental data by minimizing the discrepancies between the model predictions and the corresponding experimental data.

To explore the role of f_p in the resulting model, it was decided to check the sensitivity of the developed model predictions for the fraction of solid catalysts in the plug flow region (f_p). To achieve this goal, a number of preliminary calculations were performed. The predicted results against f_p are summarized in Table 5. These results clearly indicate that the developed model is not sensitive to this parameter (i.e., the fraction of catalyst in the plug flow region, f_p). Thus, the f_p does not play an important role in the model predictions because of the slow reaction rate of glucose to fructose and, hence, the proposed flow model could be considered only with the completely mixed region and the stagnant region. Hence, we have

$$W = W_m + W_d = (1 - f_d)W + f_d W \tag{31}$$

Therefore, the resulting model has only one adjustable parameter that is the fraction of catalyst particles remaining in the stagnant region due to the nonideal mixing in the reaction chamber. This model was applied to the experimental results and the values of the parameter obtained (i.e., f_d) are given in the figure captions.

4.2. Effect of Feed Flow Rate (q). To investigate the influence of feed flow rate on the glucose conversion, a number of experimental runs were carried out while other operating and design parameters such as the nozzle diameter, initial feed concentration, reaction chamber volume, and the catalyst loading

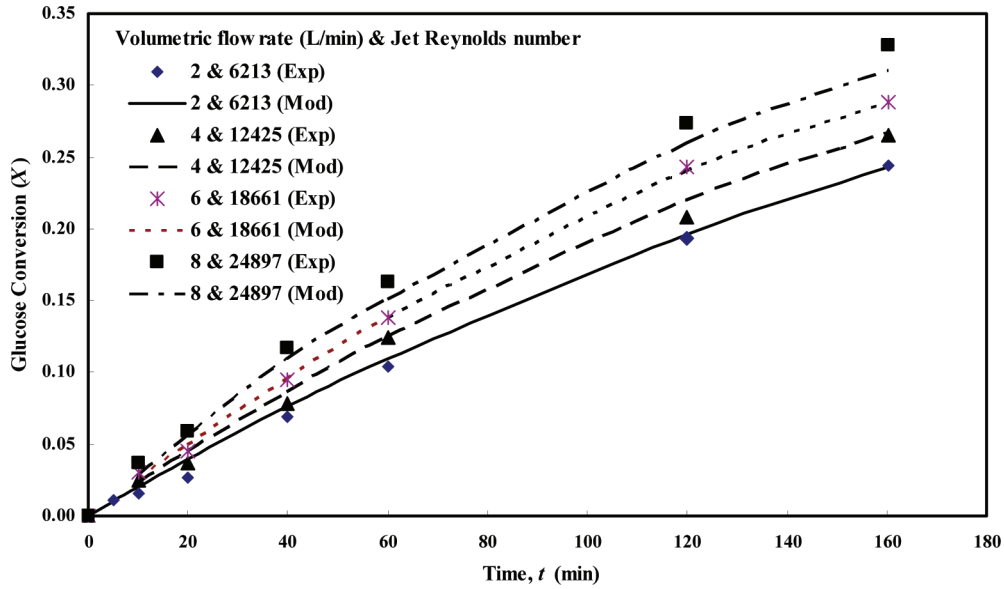

Figure 3. Effect of feed flow rate on the fractional conversion of glucose. $[G]_0 = 1250$ mol m^{-3}; internozzle distance = 1 cm; nozzle diameter = 4 mm; reaction chamber volume = 550 cm^3; catalyst loading = 10 g dm^{-3}. Obtained values of f_d: 0.3 at $q = 2$ dm^3 min^{-1}; 0.2 at $q = 4$ dm^3 min^{-1}; 0.1 at $q = 6$ dm^3 min^{-1}; 0.0 at $q = 8$ dm^3 min^{-1}.

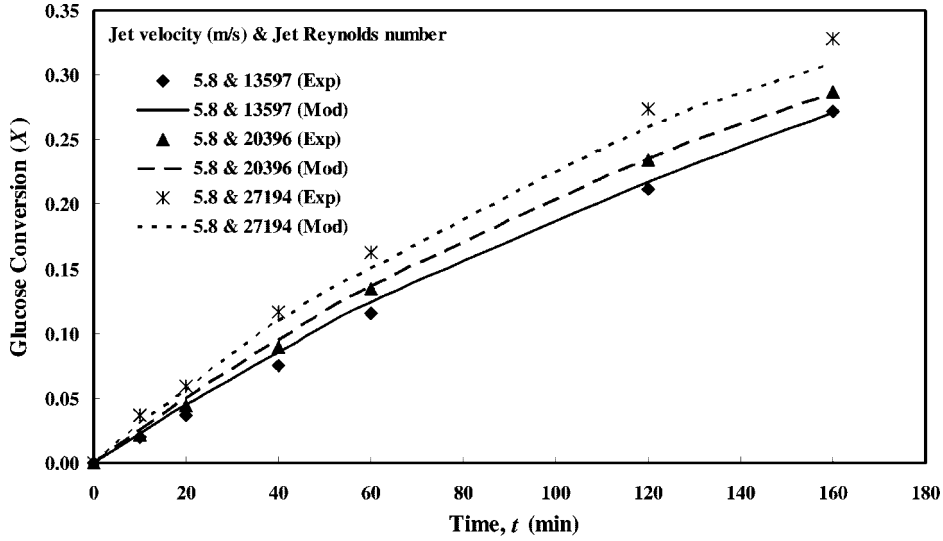

Figure 4. Effect of jet Reynolds number (Re_j) at constant jet velocity on the fractional conversion of glucose. $[G]_0 = 1250$ mol m^{-3}; internozzle distance = 1 cm; reaction chamber volume = 550 cm^3; catalyst loading = 10 g dm^{-3}. Obtained values of f_d: 0.2 at $Re_j = 13597$; 0.11 at $Re_j = 20396$; 0.0 at $Re_j = 27194$.

were kept unchanged. Figure 3 shows a plot of the fractional conversion of glucose vs time (t) as a function of the feed flow rate (q) and at the constant jet diameter, catalyst loading, and the initial feed concentration. The operating conditions of these experimental runs are given in the figure caption. As may be observed from this figure, an increase in the feed flow rate from 2 to 8 dm^3 min^{-1} leads to an increase in the fractional conversion of glucose from 0.24 to 0.33 at $t = 160$ min. This means that about 37% increase in the fractional conversion of glucose after 160 min. This increase may be attributed to (1) an increase in the jet velocity that leads to an increase in the mixing within the reaction chamber, and consequently, a decrease in the external mass-transfer resistance; and (2) a decrease in the volume of stagnant region formed within the reaction chamber due to the higher intensity of mixing within the reaction chamber. Moreover, the obtained values of f_d are given in the figure caption. These obtained values of f_d clearly support the reason given for the increase in the fractional conversion of glucose with increasing the feed flow rate.

4.3. Effect of Jet Reynolds Number (Re_j) at Constant Jet Velocity (U_j). To investigate the effect of jet Reynolds number ($Re_j = U_j d_j/\nu$) at constant jet velocity (U_j) on the performance capability of the TIJLR; a number of experiments were carried out so that the volumetric flow rate of the circulating feed was varied while the diameter of the jets was also varied in such a way that the fluid velocity exiting from the tips of the nozzles was kept unchanged at about 5.8 m s^{-1}. The experimental results obtained are illustrated in Figure 4. The operating conditions of these experiments are also given in the figure caption. As can be observed from this figure, an increase in the jet Reynolds number from 13597 to 27194 leads to an increase in the fractional conversion of glucose from 0.272 to 0.328 at $t = 160$ min. It means that about 11% increase in the fractional conversion of glucose after 160 min was obtained

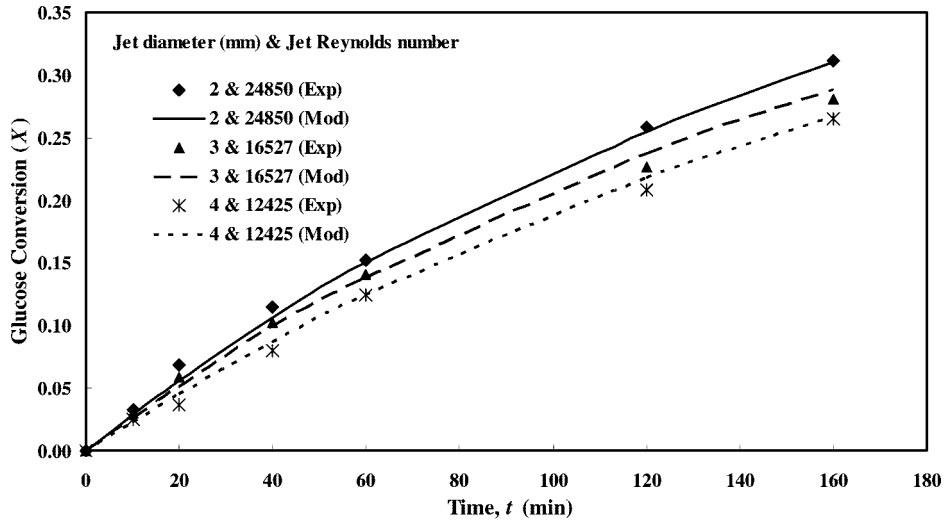

Figure 5. Effect of jet diameter on the fractional conversion of glucose. $[G]_0 = 1250$ mol m^{-3}; volumetric flow rate = 4 dm^3 min^{-1}; internozzle distance = 1 cm; reaction chamber volume = 550 cm^3; catalyst loading = 10 g dm^{-3}. Obtained values of f_d: 0.2 at $d_j = 4$ mm; 0.1 at $d_j = 3$ mm; 0.0 at $d_j = 2$ mm.

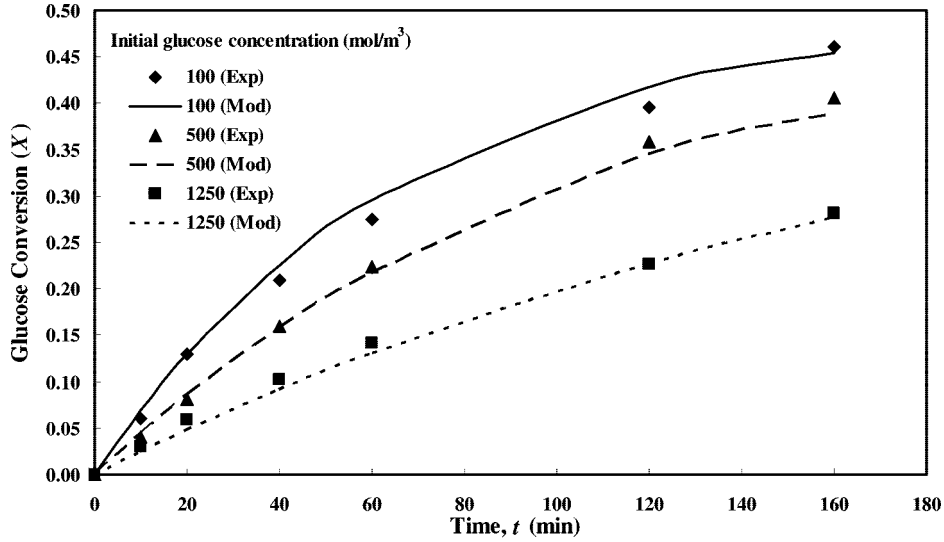

Figure 6. Effect of initial feed concentration on the fractional conversion of glucose. Nozzle diameter = 3 mm; volumetric flow rate = 4 dm^3 min^{-1}; internozzle distance = 1 cm; reaction chamber volume = 550 cm^3; catalyst loading = 10 g dm^{-3}. Obtained value of $f_d = 0.15$.

while in these experiments the jet velocity was kept constant. The superior performance of the TIJLR with increasing the Re_j values can be attributed to the fact that in this case the impinging jets produce liquid "flow" throughout the reaction chamber. The convective motion initiated by the impinging jets extends throughout the whole reaction chamber, so that at high Re_j values, the liquid and the catalyst particles within the reaction chamber are subject to the turbulent mixing action of the impinging jets and hence the possibility of any stagnant region is minimized. Note that the fraction of stagnant region (f_d) within the reaction chamber decreases from 0.20 to 0.0 with increasing Re_j value from 13597 to 27194 as given in the figure caption.

4.4. Effect of Jet Diameter (d_j). In the next step, the contribution of mixing in the reaction chamber arisen from the change in the jet diameter at constant feed flow rate on the extent of the reaction was investigated. Experiments were carried out at a constant feed flow rate of 4.0 dm^3 min^{-1} with the varying jet diameters from 2 to 4 mm. In this case, the various states of mixing are provided in the reaction chamber. As shown in Figure 5, with a decrease in the jet diameter from 4 to 2 mm at a constant feed flow rate of 4.0 dm^3 min^{-1}, the fractional conversion of glucose increases from 0.265 to 0.311 at $t = 160$ min. Such a behavior is fully expected and can be explained by increasing the mixing within the reaction chamber, consequently decreases in the external mass-transfer resistance and in the fraction of stagnant region (i.e., f_d) within the reaction chamber occur. The obtained values of f_d are given in the figure caption. The noticeable point that was observed in these experiments is that the mixing that arose from the impinging jets did not damage the catalyst particles. However, using other mechanical stirrers leads to the damage of catalyst particles and even sometimes leads to the deactivation of catalysts. Thus, for solid−liquid reaction systems whose catalysts are very sensitive to mechanical tensions, the IJ technique is a desirable means for perfect mixing and the complete elimination of external mass-transfer resistance around the solid catalyst particles.

4.5. Effect of Initial Feed Concentration ($[G]_0$). To study the influence of initial feed concentration on the performance capability of the TIJLR, a number of experiments were carried out with the various initial feed concentrations ranging from 100 to 1250 mol m^{-3} while other design and operating parameters were kept unchanged. The experimental results

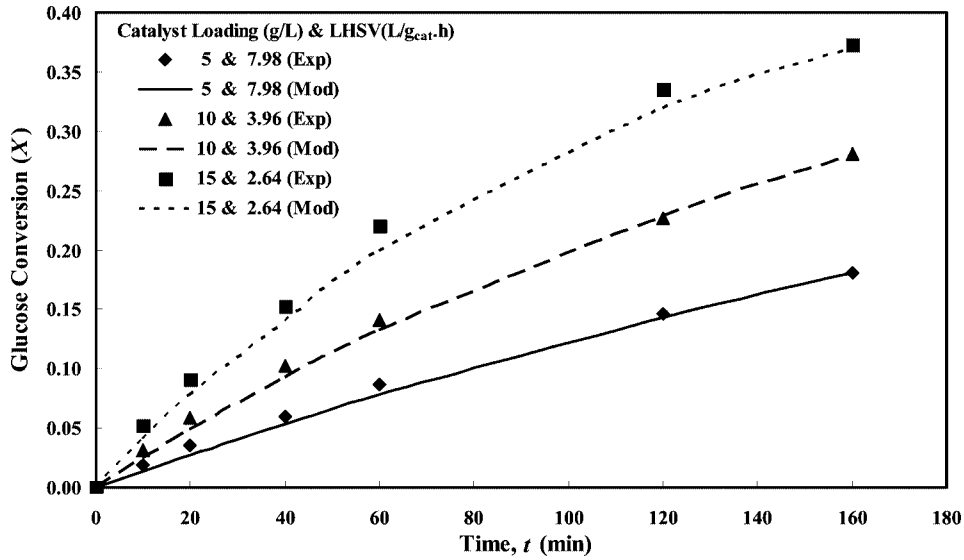

Figure 7. Effect of catalyst loading or LHSV on the fractional conversion of glucose. $[G]_0 = 1250$ mol m^{-3}; nozzle diameter = 3 mm; volumetric flow rate = 4 dm^3 min^{-1}; internozzle distance = 1 cm; reaction chamber volume = 550 cm^3. Obtained values of f_d: 0.06 at LHSV = 7.98; 0.14 at LHSV = 3.96; 0.16 at LHSV = 2.64.

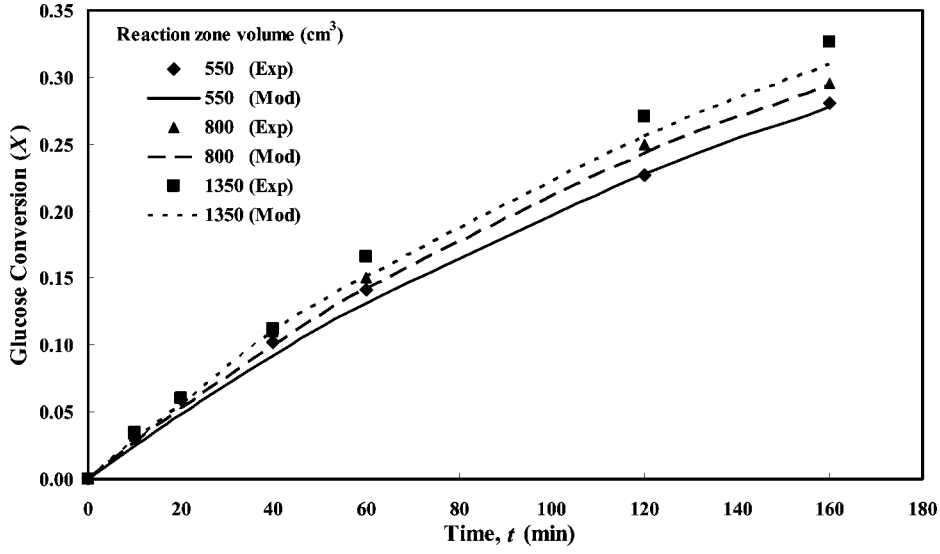

Figure 8. Effect of reaction chamber volume on the fractional conversion of glucose. $[G]_0 = 1250$ mol m^{-3}; nozzle diameter = 3 mm; volumetric flow rate = 4 dm^3 min^{-1}; internozzle distance = 1 cm. Obtained values of f_d: 0.15 at V_r = 550 mL; 0.07 at V_r = 800 mL; 0.0 at V_r = 1350 mL.

obtained are illustrated in Figure 6. The operating conditions of these experiments are also given in the figure caption. As shown in Figure 6, by increasing the initial concentration of glucose from 100 to 1250 mol m^{-3} at constant catalyst loading, the final fractional conversion of glucose decreases. This behavior is expected because the total amount of glucose in the system increases while the total amount of catalyst remains constant. As may be noticed from the figure caption, the fraction of stagnant region (f_d) in the reaction chamber for these experiments was determined, which is a constant value and equal to 0.15.

4.6. Effect of Catalyst Loading (or LHSV). To study the influence of catalyst loading on the performance capability of the TIJLR, a number of experiments with different catalyst loadings ranging from 5 to 15 g dm^{-3} corresponding to the LHSV = 7.98−2.64 (dm^3 g_{cat}^{-1} h^{-1}) were carried out while other operating conditions were kept unchanged. The experimental results of these runs are demonstrated in Figure 7. The operating conditions of these experimental runs are also given in the figure caption. As may be observed from Figure 7, by increasing the amount of catalyst loading from 5 to 15 g dm^{-3} the final fractional conversion of glucose significantly increases from 0.18 to 0.37 at the reaction time of 160 min so that the fractional conversion approaches the equilibrium fractional conversion. Considering the importance of the catalyst loading or the LHSV on the rate of glucose to fructose isomerization reaction and its important role on the performance capability of the reactor, it would be expected to observe such an intense increase in the fractional conversion after a specific time.

4.7. Effect of Reaction Chamber Volume (V_r). Finally, the effect of reaction chamber volume on the performance capability of the TIJLR was investigated. By moving the perforated plate away from or toward the impingement zone along the height of the reactor, the volume of the reaction chamber in which the feed solution contacts with the catalyst particles increases. When the perforated plate was positioned at the lowest level within the reactor, the volume of reaction chamber was set to be 550 mL. However, when the perforated plate was fitted at upper positions, we cannot change the feed flow rate freely. The latter is because that for high volumetric flow rates, the catalyst

particles are collected below the perforated plate and hence glucose solution at the bottom of the reaction chamber does not contact with the catalyst particles. However, for low volumetric flow rates of feed solution, the catalyst particles are settled down at the bottom of the reaction chamber, and hence the glucose solution at the upper section of the reaction chamber does not contact with the catalyst particles. Therefore, to achieve the conditions that the catalyst particles can contact with the glucose solution when the perforated plate is located at the upper section of the reaction chamber, we had to set the feed flow rate within a narrow range. In this case, we have a fluidized-bed reactor. In fact, by increasing the level of the perforated plate within the reaction chamber, the state of the reaction chamber changes from a mixed reactor to a fluidized-bed reactor. The experimental results obtained regarding the effect of reaction chamber volume on the performance capability of the TIJLR are illustrated in Figure 8. As may be observed from this figure, the fractional conversion of glucose increases from 0.281 to 0.326 (after 160 min) as the reaction chamber volume increases from 550 to 1350 mL. This behavior is attributed to the decrease in the stagnant region of the reaction chamber, so that the f_d value decreases from 0.15 to 0.0, with an increase in the reaction chamber volume from 550 to 1350 mL, as given in the figure caption.

5. Conclusions

A novel type of TIJLR was proposed and tested as a solid−liquid catalytic reactor. Some aspects of the behavior of the TIJLR were investigated within a range of operating and design conditions such as the jet Reynolds number, initial feed concentration, LHSV, and the volume of the reaction chamber. A compartment model with one adjustable parameter was developed to comply with the flow pattern within the reaction chamber. The experimental results were satisfactorily utilized to adjust the parameter of developed model. It was found that the parameter of the developed model (i.e., f_d) is strongly affected by the jet Reynolds number so that a rise in the latter leads to a decrease in the fraction of catalysts remaining in the stagnant region (i.e., f_d). This behavior is expected and is consistent with the state of mixing in the reaction chamber with increasing jet Reynolds number. Moreover, from the experimental results it was found that (1) the jet Reynolds number plays an important role in the performance capability of the TIJLR so that increasing the jet Reynolds number increases the fractional conversion of glucose. This behavior can be attributed to the elimination of the external mass-transfer resistance around the catalyst particles, complex flow pattern within the reaction chamber, energy released as the result of impinging-jets collision, a decrease in the stagnant region of the reaction chamber, and high intensity mixing at the impingement zone. (2) An increase in the volume of reaction chamber over the range of 500 to 1350 mL results in increasing the fractional conversion of glucose slightly. (3) The agitation promoted by this IJ technique is less aggressive than that one obtained with conventional stirrers. The latter is an important feature when sensitive particles are present in the reaction medium.

Acknowledgment

The authors gratefully acknowledge Novo Nordisk (Iran) for providing IGI catalyst and Sharif University of Technology for providing financial support.

Nomenclature

A = parameter defined in eq 22
d_j= jet diameter (m)
E = enzyme concentration (mol m^{-3})
[F] = fructose concentration (mol m^{-3})
$[F]_0$ = initial fructose concentration (mol m^{-3})
$[F]_e$ = equilibrium fructose concentration (mol m^{-3})
f_d = fraction of catalyst particles remaining in the stagnant region, unitless
[G] = glucose concentration (mol m^{-3})
$[G]_e$ = equilibrium glucose concentration (mol m^{-3})
$[G]_0$ = initial glucose concentration (mol m^{-3})
$[\bar{G}]$ = glucose concentration defined in eq 3 (mol m^{-3})
$[\bar{G}]_0$ = glucose concentration = $[G]_0 - [G]_e$ (mol m^{-3})
GE = intermediate complex defined in eq 1
K = kinetic constant defined in eq 9
K_e = equilibrium constant defined in eq 6
K_m = apparent Michaelis−Menten constant defined in eq 4 (mol m^{-3})
K_r = kinetic constant defined in eq 8 (mol g_{cat}^{-1} s^{-1})
k_{mf} = Michaelis−Menten constant for fructose (mol m^{-3})
k_{mg} = Michaelis−Menten constant for glucose (mol m^{-3})
q = volumetric flow rate of feed (m^3 s^{-1})
R = reaction rate (mol g_{cat}^{-1} s^{-1})
Re_j = jet Reynolds number = $U_j d_j / \nu$
t = time (s)
U_j = jet velocity (m s^{-1})
V = total volume of liquid (m^3)
V_d = volume of stagnant region (m^3)
V_m = maximum apparent reaction rate defined in eq 5 (mol g_{cat}^{-1} s^{-1})
V_{mx} = volume of the perfect mixed region (m^3)
V_p = volume of the perfect plug flow region (m^3)
V_r = reaction chamber volume (m^3)
υ_{mf} = maximum apparent reaction rate for fructose (mol g_{cat}^{-1} s^{-1})
υ_{mg} = maximum apparent reaction rate for glucose (mol g_{cat}^{-1} s^{-1})
W = total amount of solid catalyst (g)
W_d = amount of solid catalyst in the stagnant region (g)
W_m = amount of solid catalyst in the perfect mixed region (g)
W_p = amount of solid catalyst in the perfect plug flow region (g)
X = fractional conversion of glucose, unitless
X_e = equilibrium fractional conversion of glucose, unitless
X_m = fractional conversion of glucose at the outlet of perfect mixed region, unitless
X_p = fractional conversion of glucose at the outlet of perfect plug flow region, unitless
z = axial distance in plug flow region (m)

Greek Symbols

α, β, γ, η = parameters
ρ = fluid density (kg m^{-3})
μ = fluid viscosity (kg m^{-1} s^{-1})
ν = kinematic viscosity (m^2 s^{-1})
Δ = difference operator

Abbreviations

cal = calculated
cat = catalyst
exp = experimental
mod = model

Literature Cited

(1) Dehkordi, A. M.; Safari, I.; Karima, M. M. Experimental and Modeling Study of Catalytic Reaction of Glucose Isomerization: Kinetics and Packed-Bed Dynamic Modeling. *AIChE J.* **2008**, *54*, 1333.

(2) Asif, M.; Abasaeed, A. E. Modeling of Glucose Isomerization in a Fluidized Bed Immobilized Enzyme Bioreactor. *Biores. Technol.* **1998**, *64*, 229.

(3) Bravo, V.; Jurado, E.; Luzon, G.; Cruz, N. Kinetics of Fructose−Glucose Isomerization with Sweetzyme Type A. *Can. J. Chem. Eng.* **1998**, *76*, 778.

(4) Faqir, N. M.; Attarakih, M. M. Optimal Temperature Policy for Immobilized Enzyme Packed Bed Reactor Performing Reversible Michaelis−Menten Kinetics using the Disjoint Policy. *Biotechnol. Bioeng.* **2002**, *77*, 163.

(5) Haas, W. R.; Tavlarides, L. L.; Wnek, W. Optimal Temperature Policy for Reversible Reactions with Deactivation: Applied to Enzyme Reactors. *AIChE J.* **1974**, *20*, 707.

(6) Lee, H. S.; Hong, J. Kinetics of Glucose Isomerization to Fructose by Immobilized Glucose Isomerase: Anomeric Reactivity of D-Glucose in Kinetic Model. *J. Biotechnol.* **2000**, *84*, 145.

(7) Messing, R. A.; Filbert, A. M. An Immobilized Glucose Isomerase for the Continuous Conversion of Glucose to Fructose. *J. Agric. Food Chem.* **1975**, *23*, 920.

(8) Palazzi, E.; Converti, A. Generalized Linearization of Kinetics of Glucose Isomerization to Fructose by Immobilized Glucose Isomerase. *Biotechnol. Bioeng.* **1999**, *63*, 273.

(9) Palazzi, E.; Converti, A. Evaluation of Diffusional Resistances in the Process of Glucose Isomerization to Fructose by Immobilized Glucose Isomerase. *Enzyme Microb. Technol.* **2001**, *28*, 246.

(10) Straatsma, J; Vellenga, K.; de Willt, H. G. J.; Joosten, G. E. H. Isomerization of Glucose to Fructose. 1. The Stability of a Whole Cell Immobilized Glucose Isomerase Catalyst. *Ind. Eng. Chem. Proc. Des. Dev.* **1983**, *22*, 349.

(11) Straatsma, J.; Vellenga, K.; de Willt, H. G. J.; Joosten, G. E. H. Isomerization of Glucose to Fructose. 2. Optimization of Reaction Conditions in the Production of High Fructose Syrup by Isomerization of Glucose Catalyzed by a Whole Cell Immobilized Glucose Isomerase Catalyst. *Ind. Eng. Chem. Proc. Des. Dev.* **1983**, *22*, 356.

(12) Khorasheh, F.; Kheirolomoom, A.; Mireshghi, A. Application of an Optimization Algorithm for Estimating Intrinsic Kinetic Parameters of Immobilized Enzymes. *J. Biosci. Bioeng.* **2002**, *94*, 1.

(13) Toumi, A.; Engell, S. Optimization-Based Control of a Reactive Simulated Moving Bed Process for Glucose Isomerization. *Chem. Eng. Sci.* **2004**, *59*, 3777.

(14) Vilonen, K. M.; Vuolanto, A.; Jokela, J.; Leisola, M. S. A.; Krause, A. O. I. Enhanced Glucose to Fructose Conversion in Acetone with Xylose Isomerase Stabilized by Crystallization and Cross-Linking. *Biotechnol. Prog.* **2004**, *20*, 1555.

(15) Zhang, Y.; Hidajat, K.; Ray, A. K. Optimal Design and Operation of SMB Bioreactor: Production of High Fructose Syrup by Isomerization of Glucose. *Biochem. Eng. J.* **2004**, *21*, 111.

(16) Bailey, J. E.; Ollis, D. F. *Biochemical Engineering Fundamentals,* 2nd ed.; McGraw-Hill: New York, 1986.

(17) da Silva, E. A. B.; de Souaza, A. A. U.; de Souza, S. G. U.; Rodrigues, A. E. Analysis of the High-Fructose Syrup Production Using Reactive SMB Technology. *Chem. Eng. J.* **2006**, *118*, 167.

(18) Hong, J.; Yu, H.; Chen, K. Analysis of Substrate Protection of an Immobilized Glucose Isomerase Reactor. *Biotechnol. Bioeng.* **1993**, *41*, 451.

(19) Racki, D. V.; Pavlovic, N.; Cizmek, S.; Drazic, M.; Husadzic, B. Development of Reactor Model for Glucose Isomerization Catalyzed by Whole-Cell Immobilized Glucose Isomerase. *Bioprocess Eng.* **1991**, *7*, 183.

(20) Kikkert, A; Vellenga, K; de Wilt, H. G. J.; Joosten, G. E. H. The Isomerization of D-Glucose into D-Fructose Catalyzed by Whole-Cell Immobilized Glucose Isomerase. The Dependence of the Intrinsic Rate of Reaction on Substrate Concentration, pH and Temperature. *Biotechnol. Bioeng.* **1981**, *23*, 1087.

(21) Bower, H. Process of Facilitating Chemical Reactions. US Patent No. 410067, 1889.

(22) Elperin, I. T. Heat and Mass Transfer in Opposing Currents (in Russian). *J. Eng. Phys.* **1961**, *6*, 62.

(23) Tamir, A. *Impinging Streams Reactors: Fundamentals and Applications;* Elsevier: Amsterdam, The Netherlands, 1994.

(24) Herskowits, D.; Herskowits, V.; Tamir, A. Desorption of Acetone in a Two-Impinging-Streams Spray Desorber. *Chem. Eng. Sci.* **1987**, *42*, 2331.

(25) Tamir, A.; Herskowits, D.; Herskowits, V. Impinging-Jets Absorber. *Chem. Eng. Process.* **1990**, *28*, 165.

(26) Tamir, A.; Herskowits, D.; Herskowits, V.; Stephen, K. Two-Impinging Jets Absorber. *Ind. Eng. Chem. Res.* **1990**, *29*, 272.

(27) Kleingeld, A. W.; Lorenzen, L.; Botes, F. G. The Development and Modeling of High-Intensity Impinging Streams Jet Reactors for Effective Mass Transfer in Heterogeneous Systems. *Chem. Eng. Sci.* **1999**, *54*, 4991.

(28) Herskowits, D.; Herskowits, V.; Stephen, K.; Tamir, A. Characterization of a Two-Phase Impinging Jet Absorber: II. Absorption with Chemical Reaction of CO_2 in NaOH Solutions. *Chem. Eng. Sci.* **1990**, *5*, 1281.

(29) Dehkordi, A. M. Novel Type of Two-Impinging-Jets Reactor for Solid-Liquid Enzyme Reactions. *AIChE J.* **2006**, *52*, 692.

(30) Dehkordi, A. M. A Novel Two-Impinging-Jets Reactor for Copper Extraction and Stripping Processes. *Chem. Eng. J.* **2002**, *87*, 227.

(31) Dehkordi, A. M. Experimental Investigation of an Air-Operated Two Impinging-Streams Reactor for Copper Extraction Processes. *Ind. Eng. Chem. Res.* **2002**, *41*, 2512.

(32) Dehkordi, A. M. Liquid-Liquid Reaction with Chemical Reaction in a Novel Impinging-Jets Reactor. *AIChE J.* **2002**, *48*, 2230.

(33) Dehkordi, A. M. Liquid-Liquid Extraction with an Interphase Chemical Reaction in an Air-Driven-Two-Impinging-Streams Reactor: Effective Interfacial Area and Overall Mass-Transfer Coefficient. *Ind. Eng. Chem. Res.* **2002**, *41*, 4085.

(34) Johnson, B. K.; Prudhomme, R. K. Chemical Processing and Micromixing in Confined Impinging Jets. *AIChE J.* **2003**, *49*, 2264.

(35) Mahajan, A. J.; Kirwan, D. J. Micromixing Effect in a Two-Impinging-Jets Precipitator. *AIChE J.* **1996**, *42*, 1801.

(36) Hacherl, J. M.; Paul, E. L.; Buettner, H. M. Investigation of Impinging-Jet Crystallization with a Calcium Oxalate Model System. *AIChE J.* **2003**, *49*, 2352.

Received for review August 13, 2008
Revised manuscript received January 5, 2009
Accepted January 9, 2009

IE801240Q